THE [AN]ISOTROPY OF THE X-RAY SKY

R.A. Shafer, NASA/Goddard Space Flight Center and Dept. of Physics and Astronomy, University of Maryland, U.S.A. (currently at Institute of Astronomy, Cambridge, U.K.)
A.C. Fabian, Institute of Astronomy, Cambridge, U.K.

1. Introduction

In this presentation we show how the study of the isotropy of the X-ray sky contributes to our understanding of the structure of the universe at moderate redshifts ($1 \lesssim z << z_{recombination}$). Actually, the anisotropy of the sky flux provides the information, much as the microwave sky anisotropy does for earlier epochs. [See reports in this volume.] Though we are currently unable to make measurements with the precision and small solid angles typically achieved in the microwave, comparatively crude limits from the X-ray fluctuations place limits on the largest scale structure of the universe. We first outline the measurements of the X-ray sky and its anisotropies made with the HEAO 1 A-2 experiment. Detailed presentations are found elsewhere [Shafer 1982; Marshall et al. 1980; Piccinotti et al. 1982; Iwan et al. 1982; Shafer et al. in prep.]. We then show how the anisotropies place limits on the origin of the X-ray sky and on any large scale structure of the universe, following the example of previous analyses which used earlier anisotropy estimates [see e.g. Fabian and Rees 1978; Rees 1980; Fabian 1981].

2. The X-ray Sky

In Figure 1 we present the extragalactic sky spectrum. Several properties of the X-ray portion of the spectrum are noteworthy:

(1) It is bright. A spectrum with slope -1 in Figure 1 has equal energy per decade; thus the energy density in 3-100 keV X-rays is second only to the density of the microwave region.

(2) It is easily detected and nearly isotropic. The region from about 3 keV to ~1 MeV is the only well studied portion of the sky spectrum other than the microwave background that is not dominated by a strong galactic component.

(3) It has a well determined, if not well understood, spectrum. In terms of accuracy and bandwidth the measurement of the X-ray spectrum surpasses even determinations of the microwave spectrum [de Zotti

G. O. Abell and G. Chincarini (eds.), Early Evolution of the Universe and Its Present Structure, 333–343.

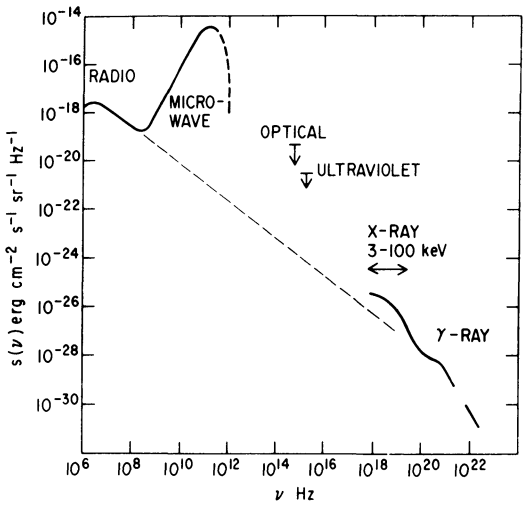

Figure 1. The Cosmic Extragalactic Spectrum. The light dashed line extends the radio discrete sources to higher energies assuming a 0.7 energy spectral index. [Radio and microwave: Longair 1978; Optical: Dube, Wickes and Wilkinson 1979; UV: Paresce, McKee and Bowyer 1980; X-ray: Marshall et al. 1980, Rothschild et al. 1983; γ-ray: Fichtel & Trombka 1981].

1982a]. The spectrum from 3 to 100 keV is well represented by a thin thermal bremsstrahlung model with a temperature of 40±5 keV [Marshall et al. 1980; Rothschild et al. 1983]. No population of sources with a single index power law spectra provides the right shape. A suitably constrained model of an evolving population with a sharp break in their spectral index is consistent with the 3-50 keV data [de Zotti et al. 1982b].

A variety of models have been presented to account for parts of the sky flux, but no coherent picture exists that satisfies all the observations. Particular models may be consistent with the data but all leave open questions or await particular observational confirmation. Known and possible fractions of the X-ray sky flux are:

(1) A galactic component. Because of the observed isotropy of the sky, any flux associated with the galactic disk can contribute no more than ~2-10% of the high galactic latitude flux, depending on the latitude of the observation [see e.g. Iwan et al. 1982]. In addition, known populations of galactic sources do not generally have the same spectrum as the sky.

(2) Well observed extragalactic sources. Based on the HEAO 1 A-2 all-sky survey the extragalactic sources resolved at high flux are predominantly either clusters of galaxies or active galactic nuclei (Seyferts, N galaxies, etc.) [Piccinotti et al. 1982]. The derived local luminosity function of these two populations can be used to estimate contributions to the total sky flux of about 4% and 18% respectively, assuming no significant evolution of the luminosity function. In addition, the low temperature thermal spectra of cluster sources [Mushotzky et al. 1978] and the power law spectra with a photon index near 1.7 typical of active galaxies do not correspond to the sky spectrum [Mushotzky et al. 1980; Rothschild et al. 1983]. In fact, no source or population has been observed to have the proper spectrum to provide the bulk of the sky emission.

(3) An evolving population of sources. This could be the evolution of

https://doi.org/10.1017/S0074180900039280 Published online by Cambridge University Press

the above known populations or the introduction of a new population of sources. QSOs, which are undergoing apparent evolution at other wavelengths, have been shown to be strong emitters in the softer 0.5 to 3.5 keV band covered by the Einstein observatory [see e.g. Zamorani et al. 1981]. Unfortunately, there are too few high quality broad band X-ray spectra of QSOs to make an unambiguous estimate of their contribution at the higher energies typical of the bulk of the X-ray sky flux. Avni [1978] pointed out that active galaxies may make up the total sky flux if they undergo only moderate evolution, in comparison to the amount of evolution suggested for QSOs in the optical. However, the evolution must involve the spectral form of the objects as well as their luminosity function [e.g. Leiter and Boldt 1982]. Suggestions for new populations of X-ray sources have included hot gas associated with the initial generation of stars of young galaxies [Bookbinder et al. 1980] and primordial black holes [Carr 1980]. Though the proposed spectra are in accordance with the X-ray sky spectrum, there have been no identifications of these new objects with observed X-ray sources.

(3) A totally diffuse component, such as a hot intergalactic medium. This model has the correct spectral form, but there are possible difficulties providing the energy to heat the medium [Field and Perrenod 1977; Fabian 1981].

Though the exact origin of the sky flux is still an open question, we have a better understanding of the principal sources of the observed anisotropy. We classify the variations in the X-ray sky intensity as large angular scale anisotropies or as fluctuations (small scale variations).

The galaxy does not dominate the 2-10 keV sky flux, but the dominant large scale variation is associated with the galactic disk. An early model of this variation was the cosecant |b| law of an infinite plane of emission [Warwick, Pye and Fabian 1980]. Other studies have noted a longitudinal component associated with the galaxy [Protheroe, Wolfendale and Wdowczyk 1980; Iwan et al. 1982]. An expected large scale anisotropy, of smaller magnitude, is a cosine or dipole anisotropy. Such a signal is expected for the same reason as the dipole variation seen in the microwave sky, i.e. motion of the observer with respect to the rest frame of the emission, the Compton-Getting effect.

The dominant contribution to the small scale fluctuations is a continuation of known source populations to lower flux levels where sources are no longer individually detectable. The size and shape of the frequency distribution of the fluctuations is a function of the number of sources versus flux relation, N(S), at those fluxes. We can explain all the fluctuations in terms of the known populations, without evolution, and place an upper bound on the size of any other small scale variations, hereafter referred to as the excess variance. This bound constrains all other sources of anisotropy. Possible origins of additional variation would be an evolving or new population of sources, or a clumping of the sources that make up the background. At the largest angular scales source clumping indicates large scale structure

in the universe, such as a global perturbation in the density $\delta\rho$. An upper bound on the excess variance limits the allowed strength of such structure, $\delta\rho/\rho$, with no assumption about the origins of the X-ray sky flux other than presuming that variations in the X-ray volume emissivity are proportional to $\delta\rho$. (For general reviews of the X-ray sky see e.g. Boldt [1981], Fabian [1981].)

3. The Data

Our results are based on measurements taken with a xenon proportional counter, one module of the A-2 experiment on the HEAO 1 satellite [Rothschild et al. 1979], taken during an all-sky survey. For the X-ray sky spectrum, 90% of the counts in this detector originate in the 2.5-13.3 keV band. We measure flux, S, in units of counts s^{-1} cm^{-2}. For typical extragalactic spectra 1 count s^{-1} cm^{-2} is equivalent to 1.35×10^{-8} ergs s^{-1} cm^{-2} (2-10 keV). The all-sky flux, S_{as}, is 58 counts s^{-1} cm^{-2}. The measured count rate depends on detector area, collimator solid angle, and integration time. For our measurements the mean sky intensity, I_{sky}, is 17.06 counts exp^{-1} (one exposure is 1.28 s). The mean count rate of the internal, non-X-ray, background is 3.5 counts exp^{-1}. The average uncertainty due to counting statistics was 0.23 counts exp^{-1}. The angular size of the measurements is fairly large, over 100 square degrees, but much of this area contributes little to the total count rate. 90% of the total comes from a rectangle of $11.2^{o} \times 4.4^{o}$, covering 49 square degrees. The central area of ~26 square degrees contributes 71% of the sky intensity but 90% of any excess variance in the intensity.

The fluctuation data were restricted to high galactic latitudes, $|b| > 20^{o}$, and free from contamination by X-ray sources in the Magellanic Clouds and bright high latitude galactic sources. When looking for large scale structure, we included data down to latitudes of 10^{o}, excluding all contamination from any resolved source cataloged in the complete all-sky sample of Piccinotti et al. [1982].

The A-2 detectors had several unique features for the continuous monitoring of internal background and determining the X-ray sky flux. The performance of the detectors, as monitored by repeat scans of the same area of the sky six months apart, was very stable. The internal background was also very stable. After selection of data to avoid noisy periods, the variation in the background was roughly 0.05 counts exp^{-1}, corresponding to a sigma 1.3% of the non-X-ray count rate and only 0.25% of the total intensity.

4. Large scale variations: Galactic and Dipole anisotropies

Using a similar set of HEAO 1 A-2 data, Iwan et al. [1982] showed that there was a variation associated with galactic longitude in addition to the latitude variation. Following that paper we fit the galactic component with a disk of finite radius and an exponential scale height. These parameters are strongly correlated and their upper bounds

poorly determined. The best fit radius was 1.8 R_{gc}, where R_{gc} is the distance from the sun to the galactic center, roughly 10 kpc. The best fit value for the scale height was 0.4 R_{gc}, with the 90% lower limit of 0.1R_{gc}, corresponding to 1 kpc, a scale typically larger than most galactic X-ray source populations. A discussion of this model and its implications is given in Iwan et al. [1982].

After removal of the best fit galactic model, we fit a dipole model, $\delta I = I_{CG} \cos \theta$, where θ is the angle between the observation and the signal maximum. The addition of this new model to the fit produced a drop in χ^2 significant at the 95% level. The strength of the signal, I_{CG}, is 0.09 ± 0.03 counts $\exp^{-1}$, about 0.5% of the sky intensity. The best fit direction in galactic coordinates, (ℓ, b), is $(282^o, +30^o)$. However the 90% confidence region for the direction is very large, covering about one eighth of the total sky. A result of similar direction, magnitude, precision, and confidence was found by Protheroe, Wolfendale and Wdoczyk [1980] using UHURU data.

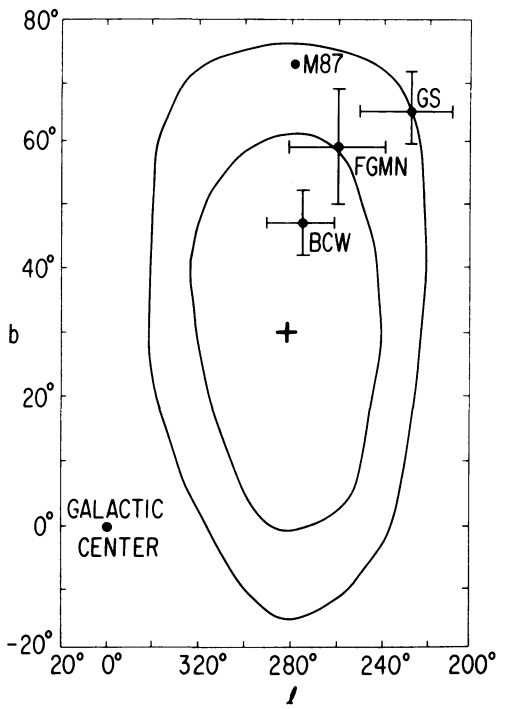

Figure 2. Position of Dipole Maximum. Contours show 70% and 90% confidence regions. The center + marks the best fit position. Also shown are the one-sigma error bars for measurements of the dipole maximum in the microwave. [BCW: Boughn, Cheng & Wilkinson 1981; FGMN: Fabbri, Guidi, Melchiorri and Natale 1980; GS: Gorenstein and Smoot 1981.]

One possible interpretation of this statistically marginal result is in terms of the Compton-Getting effect, where the size of the dipole signal is related to the observer's velocity by

$$I_{CG} = \bar{I} \, (2+\Gamma) \, v/c. \qquad [1]$$

Γ is the photon index of the sky flux, ~1.4 for the band we are interested in. The derived value for the velocity, 475 ± 165 km s^{-1}, and

https://doi.org/10.1017/S0074180900039280 Published online by Cambridge University Press

the direction are consistent with observations of the dipole signal in the microwave sky. The microwave directions in the literature are shown in Figure 2 along with the X-ray confidence regions. A synthesis performed by Wilkinson at this symposium of the different experimental results gave a best fit direction of $(265^{o},+50^{o})$ and a velocity of 372 ± 25 km s^{-1}. The origins of the Compton-Getting velocity may be responsible for an additional component of the observed X-ray dipole signal. If the velocity observed in the microwave is the integral of the acceleration caused by a large scale overdensity ("lump") at the same redshifts range at which the X-ray sky emission originates, then the lump should produce an excess in the X-ray emissivity, producing an enhancement in the direction of the lump in addition to the Compton-Getting velocity signal. Comparisons of the X-ray and microwave large-scale anisotropies help to decouple the two effects of such a lump, providing constraints on the lump's properties. [see e.g. Warwick, Pye and Fabian 1980; Fabian 1981].

The total dipole signal may be due to variations other than the Compton-Getting effect. The form of the underlying structure may not be a pure dipole. For instance, there may be second order anisotropies associated with the galaxy but not included in the finite disk model. Also, it is intriguing that the contour for the direction of the dipole maximum includes a large fraction of the local supercluster, which could provide a large scale enhancement to the sky flux. The best fit value of I_{CG} corresponds to a maximum surface brightness of 0.02 counts s^{-1} cm^{-2} sr^{-1}. The volume emissivity and total luminosity of the local supercluster required to dominate the "dipole" signal are dependent on geometry. Assuming a disk of emission centered on the dipole maximum with a radius of 4 Mpc, an estimate of the total luminosity is 2×10^{42} erg s^{-1} (H_o = 50). Previous attempts to correlate X-ray surface brightness with the local supercluster have yielded only upper limits larger than the above estimates. [see e.g. Schwartz 1980]. To test if the local supercluster is in part responsible for the fit dipole signal requires direct testing of models for the supercluster, a project now in progress. The tidal "12 hour" signal reported by Warwick, Pye and Fabian [1980] in the Ariel V data was not observed in the A-2 data.

5. Small Scale Anisotropies: The Fluctuations

Point sources have an impact on measurements of the sky flux even if the sources are too numerous to be individually resolved. The actual number of sources, and hence their total intensity, varies from one part of the sky to another. The process of extracting information about the sources from the size and shape of the intensity distributions was pioneered by radio astronomers [Scheuer 1957; Condon 1974; see e.g. Condon and Dressel 1978]. Given a model for the differential number of sources as a function of flux, N(S) dS, the distribution of intensities, $P_{I-\bar{I}}(I)$ dI, can be predicted, assuming the distribution of sources is completely random and unclumped. Standard statistical tools are used to evaluate the N(S) models by comparing the predicted distributions to observations, extending our knowledge of the X-ray

https://doi.org/10.1017/S0074180900039280 Published online by Cambridge University Press

source counts beyond what was directly accessible from resolved sources [Fabian 1975; Schwartz 1976; Pye and Warwick 1976].

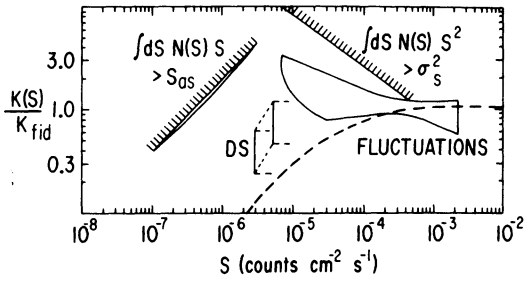

Figure 3. Number of Sources Versus Flux Derived from the Fluctuations. The plotted quantity is the ratio of the number to that expected for a fiducial Euclidean model, where $N \propto S^{-5/2}$. See text for details.

In Figure 3 we present the results of such model fitting using the HEAO 1 A-2 data. We restricted our model to a single power law form,

$$N(S)\, dS = 4\pi\, K\, S^{-\gamma}\, dS\ , \qquad [2]$$

with a sharp cutoff imposed at the low flux where the intensity contributed by the sources equals the total sky flux:

$$\int dS\, N(S)\, S = S_{as}\ . \qquad [3]$$

A population of sources distributed randomly through Euclidean space will follow a power law model with $\gamma = 5/2$. We compare an N(S) relation to the Euclidean form by defining a function K(S)

$$N(S) \equiv 4\pi\, K(S)\, S^{-5/2}. \qquad [4]$$

Figure 3 plots K(S) with respect to K_{fid}, the K value for the best fit Euclidean model, 1.48×10^{-3} (counts s^{-1} cm^{-2})$^{1.5}$. Other Euclidean models would appear on Figure 3 as horizontal lines, K(S) constant. The trumpet-shaped region on the right shows the behavior of power law models acceptable at the 90% level. The hatched line at the far left is where the power law models must be terminated to avoid exceeding the total sky flux (equation [3]). With our data, an acceptable power law model that is truncated between the hatched line and the left hand edge of the trumpet shaped region is statistically indistinguishable from the model as continued to the hatched line. The right hand edge shows the limits of the HEAO 1 resolved source counts.

The greatest constraint placed by the fluctuations is on sources roughly an order of magnitude in flux below resolved sources. However care is required in interpreting the limits on N(S). The formal validity of the confidence region rests on the assumption that the actual N(S) is well modelled by a single power law continuing without change of index past the lower limits of the region. More complicated models that do not lie wholly within the indicated region may be acceptable, e.g. the dashed line of Figure 3. This line is a schematic representation of the N(S) behavior of sources observed directly at higher fluxes and extrapolated without evolution to the lower values of

https://doi.org/10.1017/S0074180900039280 Published online by Cambridge University Press

S using the appropriate luminosity functions.

To assess the degree of source evolution at low fluxes, direct measuments of N(S) would be the easiest to interpret. The deep surveys performed with the Einstein observatory [e.g. Giacconi et al. 1979] provide such information. However information from the deep survey, indicated by the two bars labeled DS in Figure 3, also have problems of interpretation. One difficulty is in transforming source fluxes from the Einstein 1-3 keV band to the higher energy band measured in the A-2 data without good spectral information. The upper-right bar of the pair uses the published presumption that the sources have a 1.4 index power law photon spectrum, typical of the unresolved sky flux in the 2-10 keV band. The lower-left bar instead assumes that the deep survey sources have the 1.7 index spectra characteristic of active galactic nuclei. Both bars assume that N(S) is Euclidean at the deep survey flux limit. If γ were nearer that of the unevolved population's models at that flux, $\gamma \sim 1.8$, or if the sources were strongly evolving so that γ were near 3, the bars would be adjusted to 50%-130% of their indicated value. Conclusions drawn from the deep survey results must explictly consider the impact of these assumptions. Results from the Einstein medium survey [see e.g. Maccacaro et al. 1982] show source evolution less indirectly.

6. Excess Variance

The fluctuations can be totally described by models of non-evolving sources, such as the dashed line in Figure 3. The 90% upper bound to any additional variance, added as a pure Gaussian, is $\sigma^2_I \leq 0.057$ (counts $\exp^{-1})^2$. If we assume that the unevolved populations account for 20% of the sky intensity then σ_I is $\leq$1.7% of the remaining intensity. Any other source of variation is constrained by this limit.

Any evolving populations's distribution, $N_{ev}(S)$, is a source of fluctuations. It must satisfy the integral constraint

$$\sigma^2_S = \int dS\ S^2\ N_{ev}(S)\ . \qquad [5]$$

σ^2_S is a measure of the excess variance that is independent of the measurement solid angle, $\sigma^2_S \leq 7\times10^{-4}$ (counts s^{-1} $cm^{-2})^2$. The impact of this limit depends on the particular form of $N_{ev}(S)$ but if the evolved sources are to make up the remainder of the sky flux we place a lower limit on the number of sources at 75 per square degree and an upper limit on their mean flux at 1.5×10^{-5} counts s^{-1} cm^{-2} (2.0×10^{-13} erg s^{-1} cm^{-2}). If we assume that $N_{ev}(S)$ is of the form $4\pi\ K_{ev}\ S^{-3}$ we can set a limit $K \leq 1.7\times10^{-5}$ (counts s^{-1} $cm^{-2})^2$, indicated by the right-hand hatched line in Figure 3. A wide latitude for the behavior of $N_{ev}(S)$ is allowed.

These limits all assume that the sources that make up the background are not clustered, that is, their distribution among the measurements is Poisson. We can estimate that the total allowed

https://doi.org/10.1017/S0074180900039280 Published online by Cambridge University Press

variation on a scale of 26 square degrees, roughly the size of a Schmidt survey plate, is 2.3%. If QSOs contribute all of the remaining sky flux, then this limit means that the total $(\delta N/N)_{QSO} \lesssim 0.023$, where N is the mean number of QSOs on a scale of 26 square degrees, and δN is the total variation including Poisson statistics and clumping. If we assume the number of QSOs is ~200 per square degree in order to estimate the Poisson noise portion, the additional variation due to clumping can be at most 1.9%. If QSOs are observed to have clustering with a larger value of δN on these scales, then the excess variance places an upper bound on their contribution to the total sky flux.

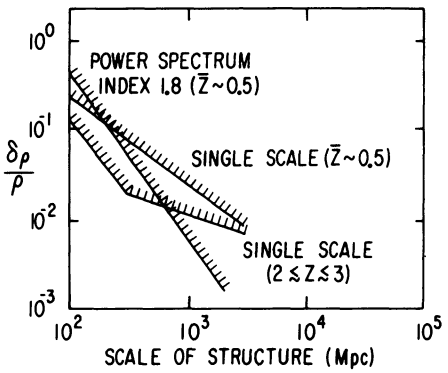

Figure 4. Preliminary upper bounds on magnitude of large scale structure from limits of X-ray excess variance.

Figure 4 shows estimates of the limits on the large scale structure of the universe placed by a previous upper bound on the excess variance. The three curves illustrate the dependence of the limits on models of the structure as well as on the origins of the X-ray sky. Two of the curves compare the case for an unevolved origin of the sky flux, $z \sim 0.5$, and the density variation restricted to a single scale or defined by a power spectrum with index 1.8, typical of the inferred distribution at smaller scales [see e.g. Peebles 1980]. The third curve is for a single scale of variation where the sky flux is dominated by an evolved component with $2 \lesssim z \lesssim 3$.

7. Conclusions

All small scale fluctuations are consistent with what we expect from known, unevolved populations of sources resolved by HEAO 1. The large scale variation, dominated by a galactic anisotropy, also admits a dipole signal which may be interpreted as a Compton-Getting dipole signal consistent with the microwave results, although other interpretations are possible. The bound on any excess variance places limits on structures at moderate redshift and of large scale otherwise not easily accessible.

We would like to thank our colleagues at GSFC, particularly C.M. Urry, for their contributions and critical advice on this presentation. ACF aknowledges the financial support of the Royal Society of London.

References

Avni, Y., 1978, Astron. Astrophys., 63, L13.
Boldt, Elihu, 1981, Comments Astrophys., 9, 97.
Bookbinder, J., L.L.Cowie, J.H.Krolik, J.P.Ostriker & M.J.Rees, 1980, Ap.J., 237, 647.
Boughn, S.P., E.S.Cheng& D.T.Wilkinson, 1981, Ap.J.(Lett.), 243, L113.
Carr, B.J., 1980, Nature, 284, 326.
Condon, J.J., 1974, Ap.J., 188, 279.
Condon, J.J., & L.L.Dressel, 1978, Ap.J., 222, 745.
de Zotti, G., 1982a, Acta Cosmol., II, 65.
de Zotti, G., E.A.Boldt, A.Cavaliere, L.Danese, A.Franceschini, F.E.Marshall, J.H.Swank & A.E.Szymkowiak, 1982, Ap.J., 253, 47.
Dube, R.R., W.C.Wickes & D.T.Wilkinson, 1979, Ap.J., 232, 333.
Fabbri, R., I.Guidi, F.Melchiorri & V.Natale, 1980, Phys.Rev.Lett., 44, 1563. (Erratum in 45, 401).
Fabian, A.C., 1975, M.N.R.A.S., 172, 149.
Fabian, A.C., & M.J.Rees, 1978, M.N.R.A.S., 185, 109.
Fabian, A.C., 1981, in Ramaty and Jones (eds.), 10th Texas Symposium on Relativistic Astrophysics, Ann.N.Y.Acad.Sci., 375, 235.
Fichtel, C.E. & J.I.Trombka, 1981, Gamma Ray Astrophysics, NASA SP-453, (Government Printing Office:Washington).
Field, G.B., & S.C.Perrenod, 1977, Ap.J., 215, 717.
Giacconi, R., J.Bechtold, B.Branduardi, W.Forman, J.P.Henry, C.Jones, E.Kellogg, H.van der Laan, W.Liller, H.Marshall, S.S.Murray, J.Pye, E.Schreier, W.L.W.Sargent, F.Seward & H.Tananbaum, 1979, Ap.J.(Lett.), 234, L1.
Gorenstein, M.V., & G.F.Smoot, 1981, Ap.J., 244, 361.
Iwan, D., F.E.Marshall, E.A.Boldt, R.F.Mushotzky, R.A.Shafer & A.Stottlemyer, 1982, Ap.J., 260, 111.
Leiter, D. & E.Boldt, 1982, Ap.J., 260, 1.
Longair, M.S., 1978, in Gunn, Longair & Rees Observational Cosmology', (Geneva Observatory:Sauverny, Switzerland).
Maccacaro, T., Y.Avni, I.M.Gioia, P.Giommi, J.Liebert, J.Stocke, J.Danziger, 1982, Ap.J., subm.
Marshall, F.E., E.A.Boldt, S.S.Holt, R.Miller, R.F.Mushotzky, L.A.Rose, R.Rothschild & P.Serlemitsos, 1980, Ap.J., 235, 4.
Mushotzky, R.F., P.J.Serlemitsos, B.W.Smith, E.A.Boldt & S.S.Holt, 1978, Ap.J., 194, 1.
Mushotzky, R.F., F.E.Marshall, E.A.Boldt, S.S.Holt & P.J.Serlemitsos, 1980, Ap.J., 235, 377.
Paresce, F., C.F.McKee & S.Bowyer, 1980, Ap.J., 240, 387.
Piccinotti, G., R.F.Mushotzky, E.A.Boldt, S.S.Holt, F.E.Marshall, P.J.Serlemitsos & R.A.Shafer, 1982, Ap.J., 253, 485.
Peebles, P.J.E., 1980, The Large-Scale Structure of the Universe, (Princeton University Press:Princeton).
Protheroe, R.J., A.W.Wolfendale & J.Wdowczyk, 1980, M.N.R.A.S., 192, 445.
Pye, J.P. & R.S.Warwick, 1979, M.N.R.A.S., 187, 905.
Rees, M.J., 1980, in Abell and Peebles (eds.), Objects at High Redshifts, I.A.U. Symp. 92, 209, (D. Reidel:Dordrecht).
Rothschild, R., E.Boldt, S.Holt, P.Serlemitsos, G.Garmire, P.Agrawal, G.Riegler, S.Bowyer & M.Lampton, 1979, Space Sci.Inst., 4, 269.
Rothschild, R.E., R.F.Mushotzky, W.A.Baity, D.E.Gruber & J.L.Matteson, 1983, Ap.J., submit.
Scheuer, P.A.G. 1957, Proc.Camb.Phil.Soc., 53, 764.
Schwartz, D.A., S.S.Murray, H.Gursky, 1976, Ap.J., 204, 315.
Schwartz, D.A., 1980, Physica Scripta, 21, 644.
Shafer, R.A., 1982, Ph.D. dissertation, University of Maryland.
Shafer, R.A., et al., 1983, in prep.
Warwick, R.S., J.P.Pye & A.C.Fabian, 1980. M.N.R.A.S., 190, 243.
Zamorani, G., J.P.Henry, T.Maccacaro, H.Tananbaum, A.Soltan, Y.Avni, J.Lieber, J.Stocke, P.A.Strittmatter, R.J.Weymann, M.G.Smith, J.J.Condon, 1981, Ap.J., 245, 357.

Discussion

Tyson: How, how often, and how well do you recalibrate the detector, and what limits does this set to the contribution of systematic errors to your claimed dipole signal?

Shafer: The data used to fit the dipole component were taken during the first nine months of satellite operations during which the experiment scanned the entire sky 1 1/2 times. The region of the dipole maximum was included in the region that was scanned twice. The detector was continually calibratable as far as pulse height gain. Gain variations were small and in any case not expected to be a major problem for the wide bandwidth measurements used to fit the dipole. The absolute sensitivity of the detector was a larger problem. The internal background was continuously monitored, while the sensitivity of the detector to X-rays could best be checked by using the sky as a reference point. By comparing measurements of the north ecliptic pole (which was measured every scan) as well as measurements of the same patch of sky (six months apart), we were able to detect a slight linear secular drift in X-ray sensitivity. In conjunction with a measured linear decrease in internal background, the total linear drift in our intensity was ~ -0.06 counts $\exp^{-1}$ in six months. Higher order variations did not have significantly better fits. We have physical models to explain the sensitivity drift. Even if we did not remove the secular drift, it would have an all-sky amplitude of about 0.1%, in comparison to the dipole measured strength of 0.5%. This is not to say that "systematics" are not important, but our current understanding of our detector, along with the independent indication from UHURU of a dipole in the same direction, indicates that the systematics associated with the actual X-ray sky (i.e., higher order galaxy contamination and/or the local supercluster) are of a greater concern than the physical performance of the detector.

https://doi.org/10.1017/S0074180900039280 Published online by Cambridge University Press